

This is a self-archived version of the original publication

The self-archived version is a publisher's pdf of the original publication. Please note that the self-archived version may differ from the original in pagination, typographical details and illustrations.

To cite this, use the original publication:

Yeshiwas, M. D., Yehualaw, M. D., Habtegebreal, B. T., Nebiyu, W. M., & Taffese, W. Z. (2025). Rice Husk Ash and Waste Marble Powder as Alternative Materials for Cement. *Infrastructures*, 10(4), 78.

DOI: <https://doi.org/10.3390/infrastructures10040078>

All material supplied via Arcada's self-archived publications collection in Theseus repository is protected by copyright laws. Use of all or part of any of the repository collections is permitted only for personal non-commercial, research or educational purposes in digital and print form. You must obtain permission for any other use.



Article

Rice Husk Ash and Waste Marble Powder as Alternative Materials for Cement

Mezgebu Debas Yeshiwas¹, Mitiku Damtie Yehualaw¹ , Betelhem Tilahun Habtegebreal¹,
Wallelign Mulugeta Nebiyu^{1,*} and Woubishet Zewdu Taffese^{2,3,*}

¹ Faculty of Civil and Water Resource Engineering, Bahir Dar Institute of Technology, Bahir Dar University, Bahir Dar 6000, Ethiopia; mezgebudebas2127@gmail.com (M.D.Y.); mitiku.damtie@bdu.edu.et (M.D.Y.); betoyet19@gmail.com (B.T.H.)

² School of Research and Graduate Studies, Arcada University of Applied Sciences, Jan-Magnus Jansson Aukio 1, 00560 Helsinki, Finland

³ Department of Civil, Architectural and Environmental Engineering, Missouri University of Science and Technology, Rolla, MO 65401, USA

* Correspondence: wallelign.mulugeta@bdu.edu.et (W.M.N.); woubishet.taffese@arcada.fi (W.Z.T.)

Abstract: Concrete, a cornerstone of modern construction, owes its widespread adoption to global industrialization and urbanization, with mortar being an essential component. However, the cement production process is energy-intensive and generates significant CO₂ emissions. This study explores the use of agricultural (rice husk ash, RHA) and industrial (waste marble powder, WMP) waste materials as partial cement replacements in mortar. Despite extensive research on RHA and WMP individually, studies examining their combined effects remain scarce. This research assessed cement replacement levels from 0% to 30% in 5% increments, evaluating the fresh, mechanical, durability, and microstructural properties of the mortar. The findings showed that replacing 20% of cement with RHA and WMP increased compressive strength by 20.65% after 28 days, attributed to improved homogeneity and pozzolanic reactions that produced more calcium silicate hydrate. Water absorption decreased from 8.3% to 6.34%, indicating lower porosity and enhanced uniformity. Microstructural analyzes showed a denser mortar with 13% less mass loss at 20% replacement level. However, higher replacement levels reduced workability due to the increased surface area of RHA and WMP. Generally, using RHA and WMP as partial replacements of up to 20% significantly enhances mortar properties and supports sustainability.

Keywords: rice husk ash; waste marble powder; fresh properties; mechanical properties; durability; microstructure; mortar; sustainability



Academic Editor: Md. Safiuddin

Received: 27 February 2025

Revised: 21 March 2025

Accepted: 27 March 2025

Published: 29 March 2025

Citation: Yeshiwas, M.D.; Yehualaw, M.D.; Habtegebreal, B.T.; Nebiyu, W.M.; Taffese, W.Z. Rice Husk Ash and Waste Marble Powder as Alternative Materials for Cement. *Infrastructures* **2025**, *10*, 78. <https://doi.org/10.3390/infrastructures10040078>

Copyright: © 2025 by the authors. Licensee MDPI, Basel, Switzerland. This article is an open access article distributed under the terms and conditions of the Creative Commons Attribution (CC BY) license (<https://creativecommons.org/licenses/by/4.0/>).

1. Introduction

Concrete, the cornerstone of modern infrastructure, plays a pivotal roles in shaping the economic progress and quality of life of nations [1]. As one of the most widely used construction materials, its inherent properties of structural stability, strength, and durability have made it indispensable in civil engineering projects. Central to concrete's production is Portland cement (PC), a material with no viable alternative in the civil construction industry, making it one of the most essential and widely produced materials globally [2]. However, cement production comes at a significant environmental cost, contributing approximately 8% global anthropogenic CO₂ emissions [3] and 12–15% of the industrial sector's global energy [4]. These emissions, along with the energy-intensive manufacturing process, have

profound implications for climate change, natural resource depletion, and environmental health [4–7]. Thus, the main opportunities in the current scenario involve replacing cements by utilizing agricultural and industrial wastes to minimize carbon footprints [3].

Researchers have been working for decades on sustainability, and recently, the pursuit of sustainable alternatives in concrete production has gained significant momentum. They have explored the potential of supplementary cementitious materials (SCMs) such as fly ash (FA), ground granulated blast furnace slag (GGBFS), silica fume (SF), rice husk ash (RHA), metakaolin (MK), and waste marble powder (WMP) as partial replacements for PC. The incorporation of these industrial and agricultural by-products has demonstrated promising results in reducing greenhouse gas emissions, energy consumption, and the ecological footprint of concrete. Furthermore, the reuse of waste materials, such as RHA and WMP, addresses pressing waste management issues, as their improper disposal often leads to environmental degradation, soil contamination, and loss of fertile land [8–11].

Among the promising SCMs, RHA and WMP have gained attention due to their distinct chemical compositions and beneficial effects on cementitious systems. RHA, a by-product of rice husk combustion, is an exceptionally reactive pozzolan with a high silica content (85–90%) and an amorphous structure that enhances the mechanical and durability properties of concrete [12]. With global rice production exceeding 600 million tons annually, the generation of millions of tons of RHA presents both an environmental challenge and an opportunity for sustainable construction [13]. With global rice production exceeding 600 million tons annually, the generation of millions of tons of RHA presents both an environmental challenge and an opportunity for sustainable construction [13]. Previous studies have demonstrated that incorporating RHA in cement mixtures at optimal replacement levels enhances compressive, tensile, and flexural strength, with improvements of up to 22.16%, 20.41%, and 22.31%, respectively [14]. Furthermore, research by Zareei et al. [15] identified 20% RHA replacement as the optimal level for enhancing compressive strength and durability, though higher replacement levels may lead to reduced mechanical performance and increased chloride ion penetration.

Similarly, WMP, a by-product of marble cutting and processing, represents a significant industrial waste problem, with disposal challenges that contribute to soil contamination, water pollution, and land degradation. However, its high calcium oxide content and inert nature make it a viable partial replacement for cement, reducing the environmental footprint of concrete while improving certain mechanical properties [11]. Lezzerini et al. [16] investigated the effects of marble powder on mortar mixes and found that replacement levels above 15% resulted in decreased compressive strength and increased water absorption. In another study, Chandrakar and Singh [17] observed that a 10% replacement of cement with marble dust powder optimized compressive strength, but higher replacement levels negatively impacted strength and workability due to increased water demand. These findings indicate that while WMP has potential as an SCM, careful optimization of its replacement levels is necessary to balance performance benefits and durability concerns.

Despite substantial research on the individual effects of RHA and WMP, limited studies have examined their combined impact in cementitious systems. Most existing investigations focus on either agricultural or industrial by-products in isolation, without assessing their potential synergy in enhancing concrete properties. Furthermore, comprehensive evaluations covering fresh, mechanical, durability, and microstructural properties remain scarce, particularly for long-term performance assessments. This research aimed to bridge that gap by systematically exploring the combined effect of RHA and WMP as partial replacements for PC in cement mortar.

Unlike prior studies that emphasize a single SCM or limited property assessments, this work undertakes a holistic approach encompassing material characterization (physical,

chemical, and mechanical properties) and extensive performance evaluations. The study employs advanced techniques such as thermogravimetric analysis (TGA), differential thermal analysis (DTA), and Fourier transform infrared (FTIR) spectroscopy to assess the microstructural development of mortar at 28 days of curing. Additionally, long-term evaluations extending to 91 days are conducted to investigate compressive strength, sulfate resistance, water absorption, and porosity. By providing a detailed understanding of the synergistic effects of RHA and WMP, this research contributes to the development of more sustainable and high-performance cementitious composites, offering a viable pathway to reducing the environmental impact of concrete production.

2. Materials and Methods

This section provides a comprehensive overview of the materials and methods employed to achieve the study's objectives. It details the selection, preparation, and characterization of the materials used, focusing on their physical, chemical, and mechanical properties. The methods adopted for material characterization are aligned with established standards to ensure reliable and reproducible results.

2.1. RHA and WMP

In this research, rice husk was collected from the Pawi agricultural farm, a region where rice cultivation is prominent. The rice husk was thoroughly cleaned to remove dust particles, sun-dried, and then burned in a controlled furnace at a temperature of 750 °C for 5 h. This process was specifically designed to produce RHA with a high content of reactive amorphous silica.

Extensive research has established the optimal burning temperatures, combustion times, and heating and cooling rates for RHA production. Generally, combustion temperatures between 500 °C and 800 °C are considered suitable [18]. Temperatures below 500 °C can leave residual organic materials in the ashes, which can adversely affect its properties. On the other hand, temperatures exceeding 800 °C cause the amorphous silica in RHA to transform into a crystalline structure, resulting in its pozzolanic reactivity and C-H produced during cement hydration [18]. Prior studies have demonstrated the impact of burning temperature on silica content. For example, RHA burned at 600 °C for 5 h yielded an 86.73% silica content [15], while burning at 750 °C achieved 93.11% amorphous silica [19]. Based on these findings, the burning temperature and time in this study were set at 750 °C for 5 h, with a controlled temperature increase rate of 15 °C per minute, to ensure maximum amorphous silica content and enhanced pozzolanic reactivity.

The waste marble powder utilized in this study was sourced from Marda Marble and Paint Production Factory which is located at Bahir Dar, Ethiopia. As an industrial by-product of marble processing, this material is typically discarded in slurry form. To prepare it for use, the slurry was sun-dried until it reached a well-dried state. Once dried, the waste marble powder was carefully collected and sieved through a 75 µm sieve to ensure consistency and suitability for the study.

2.2. Properties of Binders

To investigate the effect of RHA and WMP on cement mortar, Derba (42.5 N) OPC was selected as the base binder. This cement type was chosen due to its widespread use in local construction, serving as a benchmark for comparing the performance of RHA and WMP. Prior to investigating the impact of RHA and WMP on the cement mortar, a series of physical and chemical characterization tests were conducted on each material. These tests included determining the specific surface area, specific gravity, and chemical composition of RHA, WMP, and OPC.

The specific surface area results, as presented in Table 1, revealed that both RHA and WMP exhibit a larger specific surface area compared to OPC, suggesting a higher reactivity due to their fine particle size. However, the specific gravity of both RHA and WMP was found to be smaller than that of OPC. The high specific surface area of RHA indicates a higher reaction rate between calcium hydroxide and silica, which can contribute to increased mechanical strength of the resulting mortar [20].

Table 1. Physical properties of binders.

Materials	BET Surface Area (m ² /kg)	Specific Gravity (g/cm ³)
OPC	1000 [21]	3.15
RHA	3160.35	1.87
WMP	2938.89	2.63

According to the test results presented in Table 2, the RHA possesses a high silica content of 93.96%. This elevated silica content enables RHA to undergo a substantial pozzolanic reaction with calcium hydroxide (Ca(OH)₂), resulting in the consumption of calcium hydroxide and the formation of calcium silicate hydrate (C-S-H) gel. The C-S-H gel plays a vital role in enhancing the mechanical, durability, and microstructural properties of cement mortar. Based on ASTM C618-22 [22], RHA qualifies as a natural pozzolana. This classification is due to the fact that the combined percentage of SiO₂, Al₂O₃, and Fe₂O₃ in RHA accounts to 94.46%, which exceeds the minimum required threshold of 70% for categorization as a pozzolan. The pozzolanic activity is conventionally described as the degree of reaction over time between a pozzolan and calcium ions (Ca²⁺) or Ca(OH)₂ in the presence of water, leading to the formation of additional C-S-H gel [23]. Pozzolanic reactivity also increases with the presence of amorphous silica and depends on the fineness of particles [24]. On the contrary, WMP does not exhibit pozzolanic properties; rather, it exhibits a hydraulic nature similar to that of OPC. The maximum oxide content of WMP includes 51.82% CaO, indicating its hydraulic nature. Instead of contributing to pozzolanic reactivity, WMP primarily functions as a filler material within the composition of cement mortar [11].

Table 2. Chemical properties of binders.

Oxides	Amount of Oxides for Binders (%)		
	OPC	RHA	WMP
SiO ₂	21.03	93.96	6.08
Al ₂ O ₃	6.16	<0.01	<0.01
Fe ₂ O ₃	2.58	0.5	<0.01
CaO	64.67	0.56	51.82
MgO	2.62	0.42	0.38
Na ₂ O	0.61	<0.01	0.06
K ₂ O	0.61	0.98	<0.01
MnO	-	0.26	0.12
P ₂ O ₅	-	0.58	0.10
TiO ₂	-	0.28	0.05
H ₂ O	-	0.82	0.05
SO ₃	2.06	-	-
LOI	-	1.34	40.33
SiO ₂ + Al ₂ O ₃ + Fe ₂ O ₃	29.77	94.46	6.08

2.3. Fine Aggregates

In this study, the natural sand used for the cement mortar was sourced from Lalibela. The gradation curve for fine aggregates, determined through sieve analysis in accordance with ASTM C33 [25], is shown in Figure 1. This curve indicates that the sand complies with the upper and lower limits set by ASTM standards. Several key physical properties, including water absorption, bulk density, specific gravity, silt content, moisture content, and fineness modulus, were conducted in accordance with ASTM standards to check the suitability of fine aggregate for mortar production. The test results and the corresponding standards are summarized in Table 3.

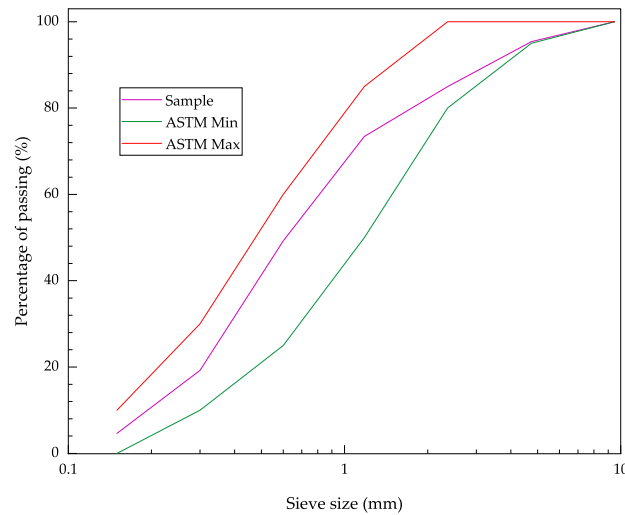


Figure 1. Gradation curve for fine aggregate.

Table 3. Physical properties of fine aggregate.

Aggregate Properties	Standard	Unit	Result	Allowable Range
Bulk density	ASTM C29 [26]	kg/m ³	1655.80	1200–1750
Specific gravity	ASTM C128 [27]	-	2.74	2.3–2.9
Fineness modules and gradation	ASTM C 33 [25]	-	2.73	2.3–3.2
Water absorption	ASTM C128 [27]	%	2.53	<5
Moisture content	ASTM C566 [28]	%	2.39	0–10
Silt content	ASTM C117 [29]	%	1.72	<5

2.4. Mix Design

The mix design for this study was developed to achieve optimal proportions of ingredients for mortar production in accordance with ASTM standards. The design incorporated fine aggregate, water, cement, and SCMs, namely RHA and WMP as a partial replacement for cement. The established mix design featured a cement-to-fine aggregate ratio of 1:2.75 and a water-to-cement ratio (w/c) of 0.49, as specified in ASTM C109 [30]. These proportions were carefully chosen to ensure the desired workability, strength, and durability characteristics of the mortar. Partial cement replacement levels ranged from 0% to 30%, incremented in 5% intervals, as indicated in Table 4.

Table 4. Proportioned materials for cement mortar.

Mix Code	% of Replacement (RHA + WMP)	Cement (kg)	RHA (kg)	WMP (kg)	Sand (kg)	Water (Liter)	Number of Cubes
Mix0	0	5.1	0	0	14.03	2.47	51
Mix5	5	4.85	0.15	0.10	14.03	2.47	51
Mix10	10	4.59	0.31	0.20	14.03	2.47	51
Mix15	15	4.34	0.46	0.31	14.03	2.47	51
Mix20	20	4.08	0.61	0.41	14.03	2.47	51
Mix25	25	3.83	0.77	0.51	14.03	2.47	51
Mix30	30	3.57	0.92	0.61	14.03	2.47	51

The freshly mixed mortar was cast into 50 mm × 50 mm cube molds to create specimens for experimental analysis. These samples were prepared to assess various performance parameters, including compressive strength (tested at 3rd, 7th, 28th, 56th, and 91th days), as well as sulfate resistance, water absorption, and ultrasonic pulse velocity (UPV) (tested at 7th, 28th, 56th, and 91th days).

2.5. Tests Conducted

A comprehensive range of tests was conducted on the cement mortar to evaluate its fresh, hardened, durability, and microstructural properties, aligning with the objectives of this research. The tests encompassed both destructive and non-destructive methods to assess critical performance characteristics of the mortar.

To assess the consistency of the paste, samples were prepared and mixed until they achieved normal consistency, defined by a Vicat plunger penetration of 10 ± 1 mm, in accordance with ASTM C187 [31]. The setting time was then measured using the Vicat apparatus, which determines both the initial setting time—the duration from water addition until the paste ceases to be fluid and plastic—and the final setting time, when the paste attains a specified level of hardness, following ASTM C191 [32].

The workability of mortar samples was evaluated using the flow table test outlined in ASTM C1437 [33]. This standardized procedure quantifies mortar flowability by placing a truncated cone of fresh mortar on a flow table, raising it to 12.7 mm, and dropping it 25 times within 15 s, after which the percentage increase in base diameter is measured.

For hardened mortar, key mechanical and durability properties were investigated, including compressive strength, water absorption, ultrasonic pulse velocity (UPV), and sulfate resistance. The mortar mixes were cast into 50 mm × 50 mm × 50 mm cubes and cured for 24 h before being demolded and submerged in water until testing. Compressive strength was tested at 3, 7, 28, 56, and 91 days following ASTM C109 [30], while water absorption, porosity, and sulfate resistance were assessed at 7, 28, 56, and 91 days following ASTM C642-06 [34] and ASTM C1012 [35]. UPV tests, conducted in accordance with ASTM C597 [36], provided non-destructive insights into the internal structure and integrity of the mortar. This technique measures the propagation velocity of vibrational energy pulses through a mortar medium [37]. A total of 15 specimens were tested for compressive strength, while 12 samples were used for the remaining tests.

To further characterize the mortar’s thermal and chemical properties, advanced analytical techniques were employed. Thermogravimetric analysis (TGA) provided quantitative measurements of mass loss due to thermal degradation, offering insights into hydration products and moisture content. Differential thermal analysis (DTA) measured temperature variations to analyze decomposition and phase transitions. Additionally, Fourier transform infrared (FTIR) spectroscopy was used to identify chemical functional groups, revealing the composition of organic, inorganic, and polymerized materials within the mortar.

Table 5 presents the tests conducted, along with the standards presented adhered to for each property.

Table 5. Tests conducted on cement mortar with standards.

Test Category	Property	Test Standard
Fresh	Workability	ASTM C1437 [33]
	Setting time	ASTM C191 [32]
	Consistency	ASTM C187 [31]
Hardened	Compressive strength	ASTM C109 [30]
	Homogeneity	ASTM C597 [36]
	Sulfate attack resistance	ASTM C1012 [35]
Durability	Absorption capacity	ASTM C642-06 [34]
	Porosity	ASTM C642-06 [34]
	Thermal decomposition	
Microstructure	Mineralogical composition	

3. Results and Discussion

3.1. Fresh Properties

3.1.1. Consistency

The normal consistency method was employed to determine the water content required for cement pastes, which would be used in subsequent tests. The results revealed that the consistency of the blended cement increased as the percentage replacement of PC with RHA and WMP increased. This phenomenon can be attributed to the higher fineness of WMP compared to PC [11] and the porous structure of RHA significantly reduced workability due to its direct water absorption [38]. As shown in Figure 2, all replacement mixtures require more water than the control mix. However, the water demand remained within the acceptable range of 26–33%, as specified by ASTM C187 [31]. The increase in water requirement can be further explained by the high specific surface area of RHA and WMP, which are significantly finer than PC. The finer particles absorb more water to form a cohesive paste, thereby increasing the consistency of the blended cement. Additionally, the increase in cement replacement levels with RHA and WMP corresponded to a proportional increase in consistency due to the finer particle size and higher specific surface area of the replacement materials compared to PC [35].

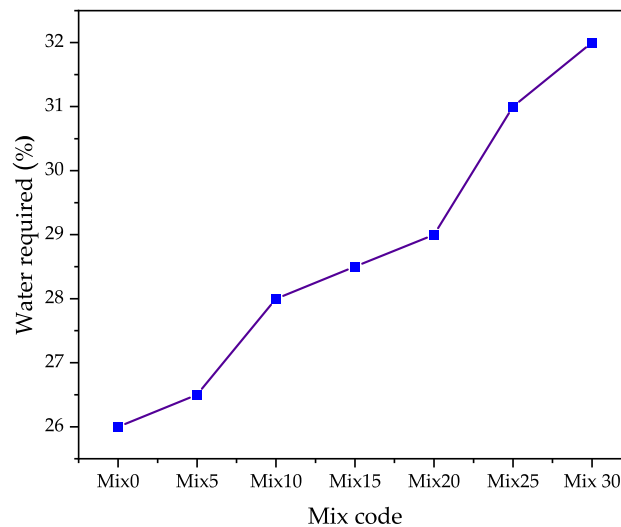


Figure 2. Consistency of cement paste containing RHA and WMP.

3.1.2. Setting Time

The setting time of cement mortars was evaluated using the Vicat apparatus, following the procedures specified in ASTM C 191 [32]. The incorporation of RHA and WMP in the mix led to significant changes in setting times. These materials, being finer than PC, increase the total specific surface area of the particles. Consequently, more water is required for wetting the particles, which accelerates the hydration reaction and reduces the setting time as the replacement percentage increases. As shown in Figure 3, both the initial and final setting times decreased with higher replacement levels of PC with RHA and WMP. This reduction in setting times is particularly pronounced for RHA, which is known to shorten the final setting time compared to other pozzolanic materials [39]. The decrease in initial setting time with higher levels of cement replacement is consistent with findings in previous studies, which have attributed this effect to the fine particle size and high reactivity of the replacement materials [40]. The observed effects can be attributed to the enhanced hydration process triggered by the finer particle size of RHA and WMP. These materials increase the reactivity of the cementitious matrix, leading to a more rapid development of hydration products and a corresponding decrease in both initial and final setting times. The initial and final setting times demonstrated a linear decrease, with reductions of up to 28% and 22%, respectively.

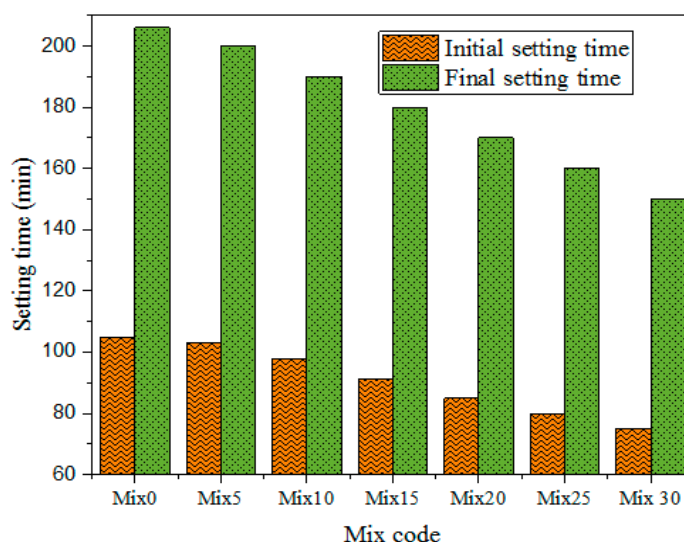


Figure 3. Setting time of cement mortars incorporating RHA and WMP.

3.1.3. Workability

The workability of the cement mortar was evaluated using the flow table test, conducted in accordance with ASTM C1437 [33]. The test requires a flow table value of 110 mm ± 5 mm, ensuring a range between 105 mm and 115 mm. The mortar was placed into the mold in three layers, compacted by tamping 20 times, followed by 25 drops of the flow table within 15 s. Figure 4 clearly illustrates that as the percentage of binder replacement (RHA + WMP) increases, the workability of the mortar progressively decreases. This reduction in slump flow can be attributed to the specific properties of RHA and WMP. RHA, being a porous material with a high specific surface area, has a pronounced water absorption capacity, which reduces the effective water available for mixing. Additionally, the irregular shape and finer particle size of the replacement materials contribute to higher water demand during the mixing process [15,41].

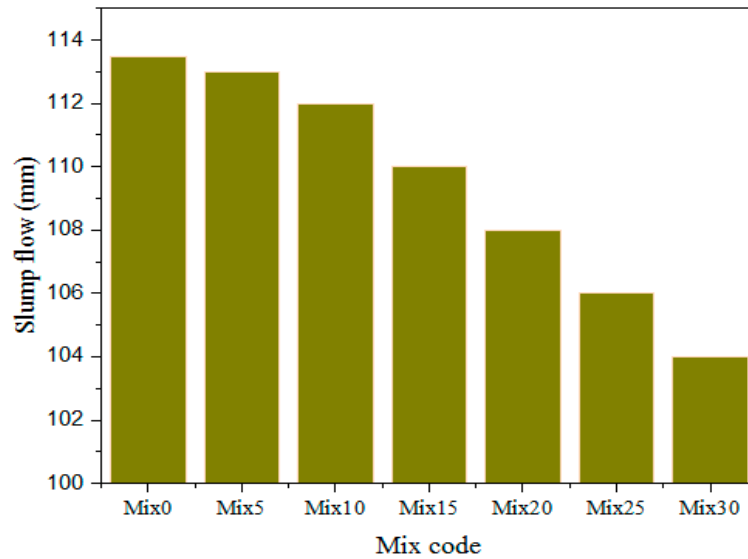


Figure 4. Slump flow of cement mortar incorporating RHA and WMP.

3.2. Mechanical Properties

3.2.1. Compressive Strength

The compressive strength of cement mortar containing RHA and WMP as partial replacements for cement was evaluated using a standard compressive strength testing machine, following ASTM C 109 [30]. Mortar cube samples were prepared for the 3rd, 7th, 28th, 56th, and 91th days. Three samples were prepared and tested for each mix at specified dates. Figure 5 illustrates the compressive strength results across various replacement levels of cement with RHA and WMP. The results reveal a significant influence of these materials on the mechanical properties of the mortar.

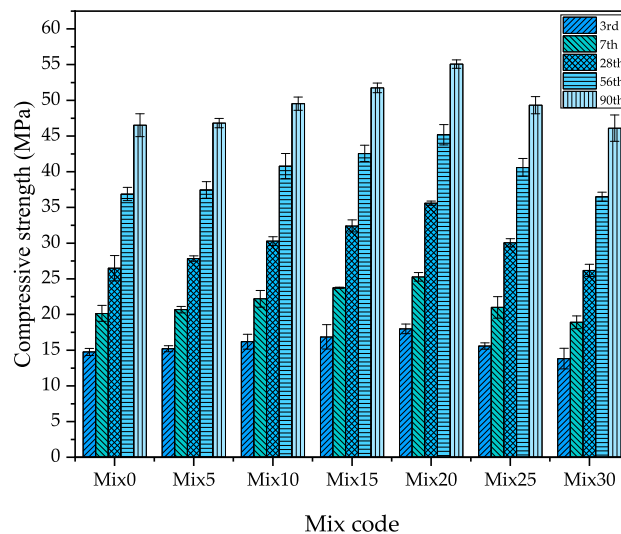


Figure 5. Compressive strength test results of cement mortar incorporating RHA and WMP.

The higher specific surface area of RHA facilitates an increase consumption of calcium hydroxide ($\text{Ca}(\text{OH})_2$) in the mortar mixture. This occurs because the high surface area of RHA accelerates the reaction between calcium hydroxide and silica, forming C-S-H bonds, which require substantial energy to break and contribute to the increased compressive

strength of the mortar [20,41]. Furthermore, the pozzolanic nature of RHA allows it to fill micro voids in the mortar matrix, enhancing its density and strength.

Similarly, waste marble powder improves compressive strength by reducing porosity within the mortar matrix through its physical properties. Additionally, WMP exhibits binding characteristics due to the hydration of calcite and C₃A (tricalcium aluminate), further improving the mortar’s structural integrity [42]. Multiple studies support the optimal replacement level of 10–15% of RHA or WMP for achieving maximum strength [41,43–45].

In this research, the compressive strength of cement mortar increased as the percentage replacement of cement with RHA and WMP rose from 0% to 20%. At 28 days of curing, the compressive strength of the control mix (0% replacement) was 27.98 MPa, while the mix with 20% replacement reached 35 MPa. However, beyond 20% replacement, the compressive strength began to decline. This reduction is attributed to limited availability of calcium hydroxide (C-H) for pozzolanic activity at higher cement replacement levels. Additionally, the formation of C-S-H gel diminished as more cement was replaced, leading to reduced mechanical strength [15,20,38,46].

3.2.2. Ultrasonic Pulse Velocity

Figure 6 displays the results of the UPV test. For this study, 50 × 50 × 50 mm mortar cubes were prepared, with three specimens tested at each evaluation date. The UPV results indicated that the optimal UPV value was achieved when cement was replaced with 20% of RHA and WMP across the range of 0% to 20% replacement levels. As shown in Figure 5, the UPV test results demonstrate a consistent trend of increasing values with higher percentages of cement replacement in the mortar mixes of up to 20%. Specifically, after 28 days of curing, laboratory measurements recorded velocities of 3.1 km/s for 0% replacement and 3.5 km/s for 20% replacement.

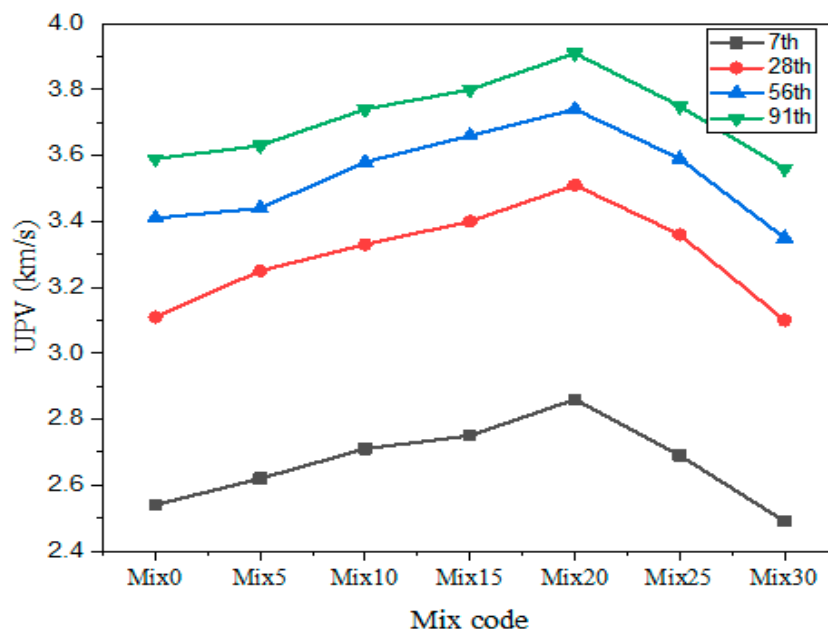


Figure 6. Results of the UPV test for cement mortar incorporating RHA and WMP.

3.3. Microstructure Properties

3.3.1. Thermogravimetric Analysis

Thermogravimetric analysis (TGA) is a widely utilized method for characterizing materials by measuring their mass changes as a function of temperature. This method offers invaluable insights into the degradation rates, moisture content, and thermal stability

of materials. TGA quantifies mass variations associated with the thermal degradation of a sample, providing precise measurements of mass loss during heating. When cement-based materials are subjected to elevated temperatures, the hydration products undergo thermal decomposition, releasing water vapor and carbon dioxide. The TGA apparatus measures these changes in mass in real-time, enabling accurate calculation of mass loss throughout the thermal process [47].

The decomposition of cement hydrates during TGA is generally observed in three distinct stages. The first stage, occurring between 25 °C and 105 °C, is characterized by the loss of free water. Following this, between 105 °C and 400 °C, the hydration products undergo dehydration. In the second stage, from 400 °C to 600 °C, Mix0 and Mix20 experience significant mass loss in this range. This mass loss corresponds to the thermal decomposition of calcium hydroxide (Ca(OH)₂) into calcium oxide (CaO) and water vapor. The third and the final stage corresponds to decarbonation of CaCO₃ from 600 °C to 800 °C, where the material releases carbon dioxide (CO₂) upon heating. These stages provide a clear indication of the thermal behavior of cement-based materials under varying temperature conditions [48].

Figure 7 presents the TGA results, showing the mass loss at 28 days of curing for three selected mix compositions: Mix0, Mix20, and Mix30. These mixes were chosen based on their divergent compressive strength trends, with Mix 0 serving as the baseline, Mix20 exhibiting optimal strength, and Mix30 demonstrating inferior performance. The TGA data reveal critical insights into the relationship between cement replacement levels, hydration products, and mechanical behavior. Notably, Mix30 exhibits the highest total mass loss (8.6%), significantly exceeding that of the control mix (6.5%) and Mix20 (6.4%). This elevated mass loss in Mix30 suggests reduced structural stability, likely due to incomplete pozzolanic reactions or excessive cement dilution, which aligns with its inferior compressive strength. In contrast, Mix20 demonstrates the lowest mass loss, underscoring its enhanced microstructure and chemical stability.

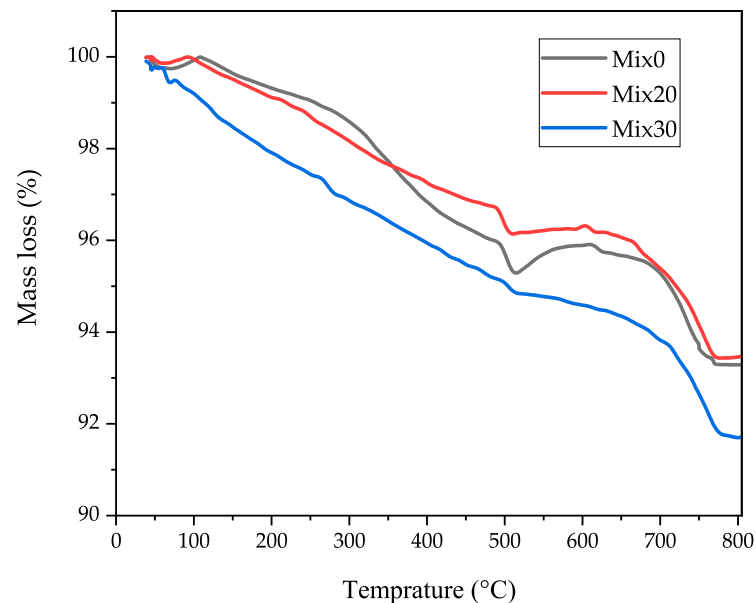


Figure 7. TGA at 28 days of curing for cement mortar containing RHA and WMP.

A key thermal event occurs within the temperature range of approximately 450–550 °C, primarily corresponding to the decomposition of C-H due to the dehydration of Ca(OH)₂. The control mix exhibits higher mass loss in this range compared to Mix20. The reduced

C-H mass loss in Mix20 can be attributed to the pozzolanic reaction, where highly reactive silica from RHA reacts with $\text{Ca}(\text{OH})_2$, forming additional C-S-H gel. This observation aligns with the mechanical performances discussed earlier. Additionally, Mix20 exhibits higher mass loss in the 0–450 °C range, further supporting the increased formation of C-S-H gel [3,49].

The superior performance of Mix20 is thus linked to its optimized pozzolanic activity at 20% cement replacement. The reactive silica in RHA effectively consumes calcium hydroxide, mitigating its deleterious effects while generating additional C-S-H gel. This densification enhances mechanical strength, durability, and long-term stability. Conversely, the inferior performance of Mix30 likely stems from an imbalance in the binder-to-pozzolan ratio, where excessive replacement disrupts hydration kinetics, leaving unreacted constituents and weakening the matrix [48].

3.3.2. Differential Thermal Analysis

Differential thermal analysis is a valuable thermal analysis technique used to investigate the thermal behavior and properties of materials. It measures the temperature difference between the sample and a reference material as they undergo controlled heating or cooling. This technique provides critical information about phase transitions, thermal stability, decomposition, and other thermal events. In particular, DTA is useful for observing changes in material composition during heating, including the decomposition of compounds and the occurrence of exothermic and endothermic reactions. Notably, the peak associated with the decarbonation of calcium carbonate is completely absent when the sample is heat-treated to 800 °C, which aligns with expectations [50].

Figure 8 presents the DTA curve for the cement mortar samples at 28 days of curing, with varying levels of cement replacement: 0%, 20%, and 30%, using RHA and WMP. Decomposition of calcium hydroxide ($\text{Ca}(\text{OH})_2$) occurs in the temperature range of 450–710 °C, while calcium carbonate (CaCO_3) decomposes between 710–1020 °C. Additionally, the evaporation of absorbed water is observed around 35–140 °C. An exothermic reaction, occurring between 140 and 400 °C, can be attributed to the presence of C-S-H, a critical component in cement hydration [51].

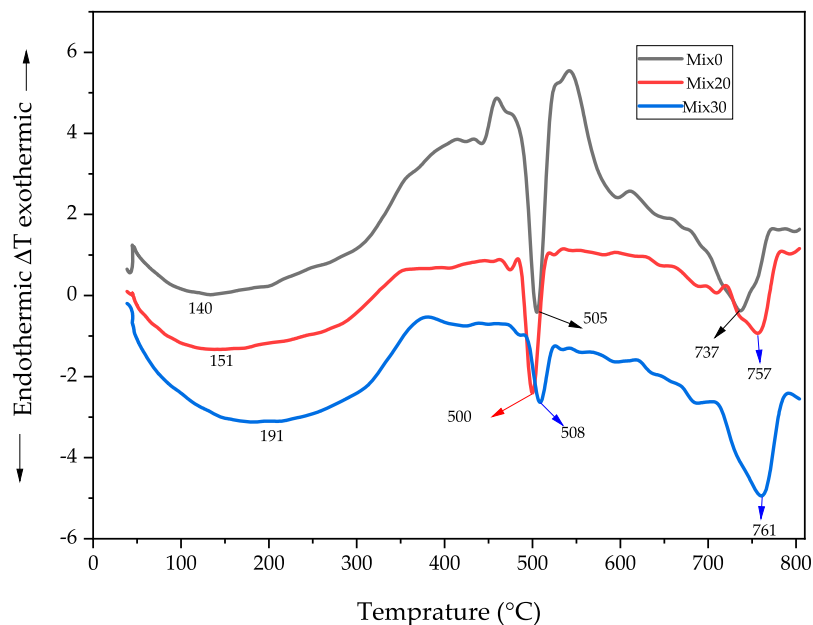


Figure 8. DTA curve at 28 days of curing for cement mortar containing RHA and WMP.

As shown in the DTA curves, the endothermic peaks associated with the decomposition of calcium hydroxide appear at 505 °C, 500 °C, and 508 °C for 0%, 20%, and 30% replacement, respectively. In contrast, the exothermic peaks corresponding to the breakdown of C-S-H gel occur at 414 °C, 357 °C, and 378 °C for 0%, 20%, and 30% replacement, respectively. These shifts in thermal behavior demonstrate the influence of the RHA and WMP additives on the thermal properties of the cement mortar, highlighting differences in hydration and decomposition patterns.

3.3.3. Fourier Transformation Infrared Spectroscopy

Fourier transform infrared spectroscopy (FTIR) analysis of hardened mortar was conducted to examine the potential of chemical changes resulting from the addition of admixtures. This analysis identified the presence of organics, such as OH hydroxyl groups, C-O-C stretching vibrations [52]. In FTIR analysis, infrared radiation is passed through the sample, with some radiation being absorbed and some transmitted. The resulting spectrum represents the molecular absorption and transmission, creating a molecular fingerprint of the sample. This fingerprint can be used to identify unknown materials, assess the quality or consistency of the sample, and determine the composition of mixture [41]. According to [47], FTIR is a method for identifying chemical functional groups in a product, where the specific wavelengths absorbed are characteristic of the chemical groups present in the analyzed material. The measurements were carried out using an IRAFFINITY-1 apparatus, with a scanning range between 400 and 4000 cm^{-1} , 40 scans, and a resolution of 4 cm^{-1} . The main characteristic peaks of C-S-H are located in the range of 1100–900 cm^{-1} [53].

Figure 9 presents the FTIR spectra for cement mortar samples with 0%, 20%, and 30% replacement of cement by RHA and WMP after 28 days of curing. The peak absorption bands for C-S-H were observed at 963 cm^{-1} , 969 cm^{-1} , and 960 cm^{-1} for 0%, 20%, and 30% replacement, respectively, with broader bands ranging between 1196 and 747 cm^{-1} , 1222 and 755 cm^{-1} , as well as 1196 and 886 cm^{-1} . Among these, the 20% replacement exhibited the broadest and strongest bands, indicating a higher formation of C-S-H gel due to increased pozzolanic activity. The strong asymmetric bending at 900–1100 cm^{-1} corresponds to the formation of hydration products, including calcium silicate hydrate C-S-H, in the lime composite mortars [54].

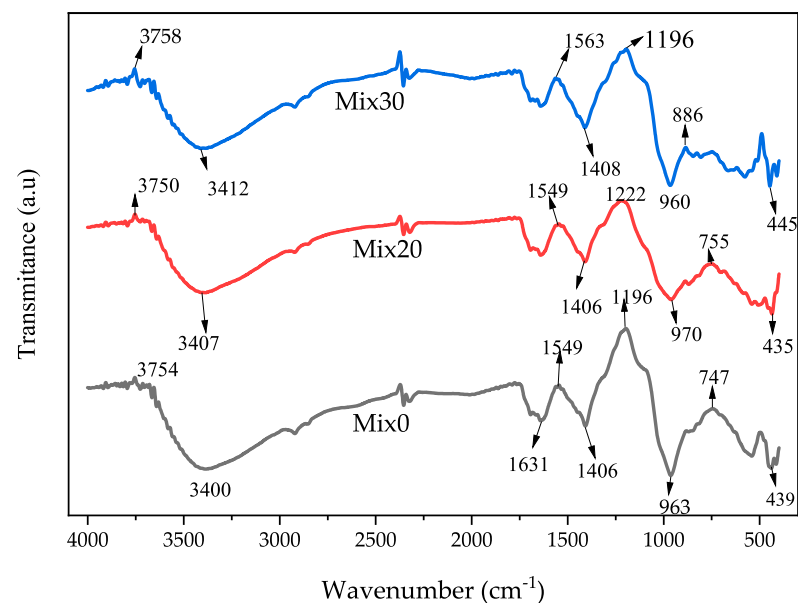


Figure 9. FTIR spectra of cement mortar containing RHA and WMP at 28 days of curing.

The FTIR spectra of C-S-H shifted to lower wave numbers, reflecting a decrease in polymerization. Conversely, shifts to higher wave numbers were attributed to silica polymerization during the decalcification process. This method also highlights the shifts in bands assigned to C-S-H under curing and aging conditions [53]. The carbonate peak absorption bands for 0%, 20%, and 30% replacement were observed at 1406 cm^{-1} , 1406 cm^{-1} , and 1408 cm^{-1} , respectively, with ranges of $1549\text{--}1196\text{ cm}^{-1}$, $1549\text{--}1222\text{ cm}^{-1}$, and $1563\text{--}1196\text{ cm}^{-1}$. The narrower band for the 20% replacement indicates a reduction in carbonate formation. Additionally, the infrared absorption bands of calcite at 1421 cm^{-1} shifted to 1448 cm^{-1} , likely due to crystal deformation of calcium carbonate (CaCO_3) caused by organic materials in the mortar [55].

The peak and range values of OH groups were recorded at 3400 cm^{-1} , 3407 cm^{-1} , and 3412 cm^{-1} for 0%, 20%, and 30% replacement, respectively, with band ranges of $3754\text{--}2967\text{ cm}^{-1}$, $3750\text{--}2957\text{ cm}^{-1}$, and $3758\text{--}2986\text{ cm}^{-1}$. Peak areas corresponding to carbonates were observed in the interval of $1300\text{--}1700\text{ cm}^{-1}$ in the original spectra without subtraction, while the OH-stretching region appeared above 3000 cm^{-1} [56]. A broad absorption band formed from 30% cement replacement with RHA and WMP in the OH group region, as indicated in the graph.

3.4. Durability Properties

3.4.1. Sulfate Attack Resistance

Sulfates react with the hydrated calcium aluminates in cement to form calcium sulphoaluminates, which expand in volume compared to the original aluminates. Additionally, sulfates react with free calcium hydroxides in cement to form gypsum and ettringite, which lead to various forms of deterioration, such as spalling, cracking, softening, expansion, and strength loss [57].

To evaluate sulfate resistance, mortar cubes were prepared and immersed in a sodium sulfate solution (5% by weight) instead of water curing. The cubes were tested at specified intervals (7, 28, 56, and 90 days). Compressive strength tests were conducted, and the results revealed the impact of sulfate attack on the samples. The findings indicate that sulfate resistance improved as the cement replacement percentage with RHA and WMP increased, peaking at 20% as shown in Figure 10. The enhanced resistance can be attributed to the finer particle size of RHA and WMP, which reduces overall porosity by transforming continuous pores into discontinuous ones. This densification decreases permeability, limiting sulfate ion ingress and reducing the number of reactive sites for sulfate attack. Furthermore, the pozzolanic properties of RHA play a crucial role. The reaction between RHA and calcium hydroxide produced during cement hydration generates additional C-S-H gel, resulting in a denser and more sulphate-resistant microstructure [45].

As shown in Figure 11, the compressive strength reduction caused by sulfate attack decreased with up to 20% cement replacement. This is due to adding RHA to the mortar making it better at resisting damage from sodium sulfate because of RHA has much less aluminum, which helps prevent the harmful reactions that cause expansion and cracking in concrete [57]. Beyond its influence on aluminum oxide (Al_2O_3) content, the physical characteristics and pozzolanic properties of RHA are critical for enhancing sulfate resistance. The pozzolanic reaction occurs when RHA interacts with the calcium hydroxide generated during cement hydration, leading to the formation of additional calcium silicate hydrates (C-S-H). This process results in a denser and more resilient cementitious matrix that is better equipped to withstand sulfate attacks [45]. For instance, at 28 days of curing, the strength reduction was 1.11 MPa for 0% replacement and 0.78 MPa for 20% replacement. However, beyond the 20% replacement level, sulfate resistance began to decline, with the lowest resistance observed at 30% replacement. This decrease may be due to excessive

replacement altering the mortar’s composition and pore structure, thereby reducing its resistance to sulfate attack.

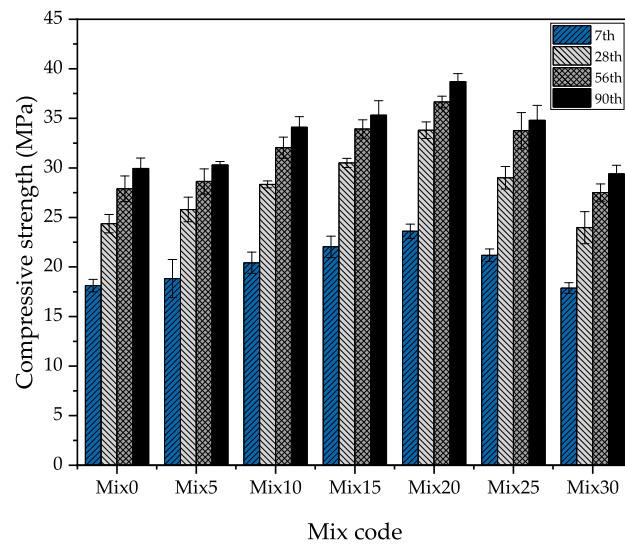


Figure 10. Compressive strength of mortar samples after immersion in sulfate solution at varying curing days.

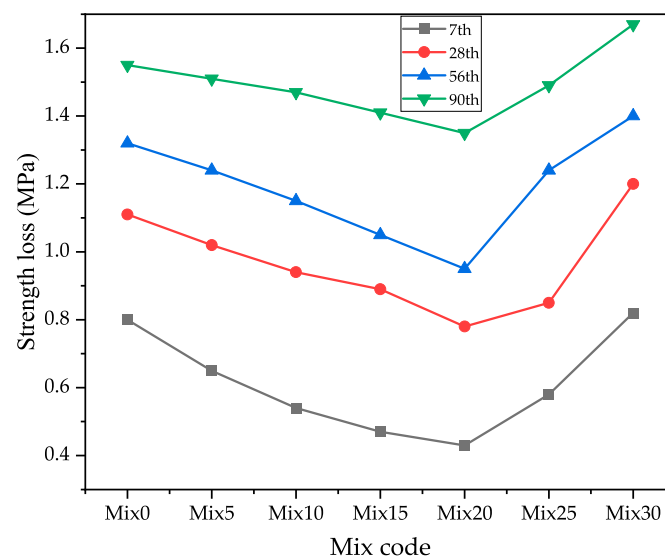


Figure 11. Compressive strength reduction of mortar samples due to sulfate attack at varying curing days.

3.4.2. Water Absorption

Research has consistently demonstrated that blended cement mortar exhibits significantly lower permeability compared to non-blended counterparts. This enhancement in absorption properties can largely be attributed to the pozzolanic reaction induced by RHA. The high silica content in RHA reacts with calcium hydroxide, a by-product of cement hydration, to form C-S-H gel. This gel improves the microstructure by refining the pore system, resulting in enhanced water resistance. As the replacement percentage of RHA and WMP increases, the pore system transitions from an open structure to a more closed-pore system, significantly reducing permeability. However, this leads to a reduction in OPC content, subsequently decreasing the hydration products within the mortar. This reduc-

tion, combined with the filler effect of pozzolans, contributes to altered water absorption characteristics [37].

As illustrated in Figure 12, the optimal replacement level to minimized water absorption was found to be 20%. At this replacement level, the water absorption at 28 days of curing was reduced to 6.34%, compared to 8.3 in the control mix sample. Similarly, at 91 days, water absorption decreased to 5.85% at 20% replacement, compared to 7.46% in the control sample. This finding aligns with the results of [58] which reported a 16.3% reduction in water absorption when 20% RHA replaced cement and 30% MWP substituted fine aggregate. The significant reduction is attributed to the synergistic effects of the pozzolanic reaction, additional C-S-H gel formation, and pore refinement. However, beyond the 20% replacement threshold, water absorption begins to increase, with the maximum water absorption at 30% replacement level, surpassing that of the control sample.

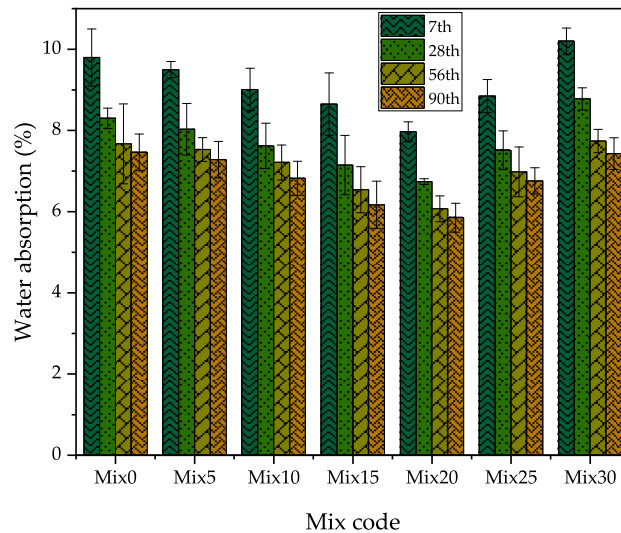


Figure 12. Water absorption of mortar samples at varying curing days.

3.4.3. Porosity

Blended cements have gained global acceptance for their ability to generate more uniform hydration products, leading to the segmentation and filling of capillary voids, ultimately resulting in denser and less permeable mortar. As the percentage of replacement materials increases, a notable reduction in total porosity is observed [59]. The incorporation of blended cement enhances the packing efficiency of the cementitious matrix, reducing void spaces and improving the interconnectivity between cement particles. Replacement materials, such as pozzolans or fillers like RHA and WMP, significantly contribute to pore refinement and porosity reduction. The pozzolanic activity of RHA, in particular, accelerates the formation of additional hydration products, leading to a more homogenous and refined microstructure.

The experimental results reveal that the porosity of cement mortar cubes containing RHA and WMP decreases with increasing replacement percentages up to 20%, as shown in Figure 13. This result is also supported by researchers that state that the porosity and sorptivity of the concrete material were reduced when cement is replaced by up to 15–30% RHA and WMP [37,60]. Specifically, the porosity is reduced from 16.22% to 13.28% at 28 days of curing and from 15.53% to 12.52% at 91 days of curing as the replacement level increased from 0% to 20%. This reduction is attributed to the pozzolanic activity of RHA, which reacts with calcium hydroxide to generate additional hydration products, and the

filler effect of RHA and WMP, whose fineness surpasses that of cement. These factors enhance pore refinement and reduce overall porosity.

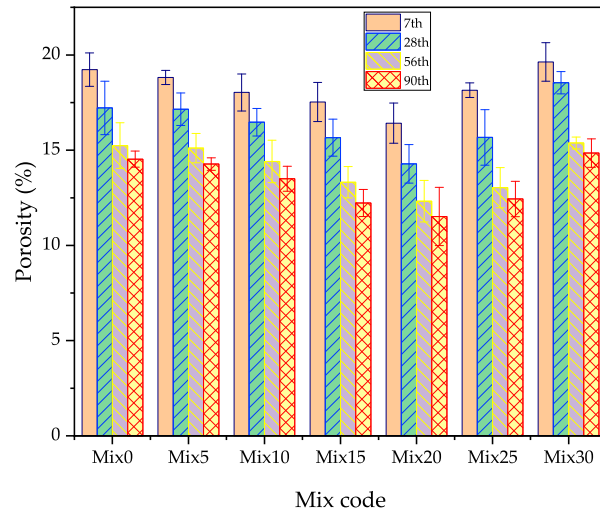


Figure 13. Porosity of mortar samples at varying curing days.

The optimum porosity reduction was achieved at the 20% replacement level. However, beyond this threshold, the porosity began to increase, suggesting that excessive replacement of cement with RHA and WMP compromises the hydration process by reducing the amount of available hydration products. Consequently, the 30% replacement level exhibited a porosity value higher than that of the control sample.

3.5. Correlation Analysis

The relationships among compressive strength, water absorption, ultrasonic pulse velocity, and porosity were analyzed using the experimental data, as illustrated in Figure 14. A strong correlation was observed between compressive strength and UPV, with a coefficient of determination (R^2) of 0.9866, indicating a direct and significant relationship. This strong correlation reflects the homogeneity of the mortars and confirms that as compressive strength increases, UPV values also increase, demonstrating the densification and integrity of the cementitious matrix.

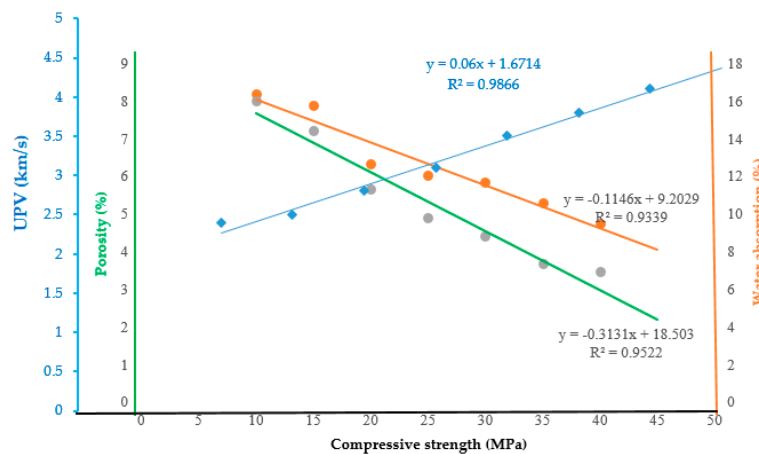


Figure 14. Correlation among compressive strength, water absorption, UPV, and porosity of mortar samples.

In contrast, water absorption and porosity exhibited an indirect (negative) correlation with both compressive strength and UPV. The R^2 value for the relationship between water absorption and compressive strength was 0.9339, while the correlation between porosity and compressive strength yielded an R^2 of 0.9522. These findings highlight the inverse relationship between porosity, water absorption, and the mechanical and structural properties of the mortar. Specifically, as the compressive strength increases, both water absorption and porosity decrease exponentially, underscoring the significant role of pore refinement in enhancing the durability and strength of the material [2,61,62]. These strong correlations reinforce the importance of optimizing cementitious compositions to achieve improved performance in terms of strength, durability, and impermeability.

4. Conclusions

This study aimed to investigate the agricultural (rice husk ash) and industrial (waste marble powder) waste materials as partial replacements for cement in the production of cement mortar. To ensure suitability, the physical properties (specific surface area and specific gravity) and chemical composition of the materials were analyzed. According to ASTM C618-22, RHA was categorized as a natural pozzolana due to its high silica content (93.96%) after being burned at 750 °C for 5 h, while WMP, predominantly composed of CaO, was classified as a non-pozzolanic material. Key findings of this research are as follows:

- **Workability and setting time:** The incorporation of RHA and WMP led to reduced workability and shorter setting times, attributed to their higher specific surface area compared to cement. The initial and final setting times exhibited a linear decline, with reductions of up to 28% and 22%, respectively. Additionally, workability decreased by 9.25% at 30% replacement (Mix30).
- **Mechanical properties:** Compressive strength and UPV improved with replacement levels up to 20%, due to the formation of additional C-S-H gel, which enhanced matrix uniformity and densification. At 20% replacement (Mix20), compressive strength reached its peak increase of 26.33%, while UPV improved by 9.44% after 90 days of curing compared to the control mix. However, beyond 20% replacement, a decline in both compressive strength and UPV was observed, indicating a loss of matrix homogeneity.
- **Durability:** Sulfate resistance significantly improved with increasing replacement levels, peaking at 20% replacement due to pore refinement, reduced porosity, and enhanced C-S-H formation. The inclusion of RHA and WMP resulted in a 12.9% increase in sulfate resistance at Mix20 after 91 days compared to the control mix. Additionally, water absorption and porosity were at their lowest at 20% replacement; however, beyond this level, both properties increased, suggesting a threshold for optimal durability performance.
- **Thermal and structural analysis:** TGA demonstrated minimum mass loss in hardened mortar at 20% cement replacement. The FTIR analysis corroborated these findings, revealing a denser internal structure with increased C-S-H formation and a reduction in C-H as the replacement percentages rose to 20%.

In conclusion, the optimal replacement level of cement with RHA and WMP was determined to be 20%, providing the best balance between strength, durability, and uniformity. This study highlights the potential of utilizing agricultural and industrial waste materials to enhance the sustainability of cementitious systems, offering a viable solution for waste management and resource efficiency in the construction industry.

Author Contributions: Conceptualization M.D.Y. (Mezgebu Debas Yeshiwas) and M.D.Y. (Mitiku Damtie Yehualaw); methodology, M.D.Y. (Mezgebu Debas Yeshiwas) and M.D.Y. (Mitiku Damtie

Yehualaw); software, W.M.N. and M.D.Y. (Mezgebu Debas Yeshiwas); validation, M.D.Y. (Mezgebu Debas Yeshiwas), W.Z.T. and M.D.Y. (Mitiku Damtie Yehualaw); formal analysis, M.D.Y. (Mitiku Damtie Yehualaw) and W.Z.T.; investigation, M.D.Y. (Mezgebu Debas Yeshiwas), B.T.H. and M.D.Y. (Mitiku Damtie Yehualaw); resources, M.D.Y. (Mezgebu Debas Yeshiwas) and B.T.H.; data curation, W.M.N. and W.Z.T.; writing—original draft preparation, M.D.Y. (Mezgebu Debas Yeshiwas) and W.M.N.; writing—review and editing, W.Z.T., M.D.Y. (Mitiku Damtie Yehualaw) and W.M.N.; visualization, W.Z.T. and B.T.H.; supervision, M.D.Y. (Mitiku Damtie Yehualaw). All authors have read and agreed to the published version of the manuscript.

Funding: This research received no external funding.

Data Availability Statement: Data are contained within the article.

Acknowledgments: The authors sincerely appreciate the support of the Faculty of Civil and Water Resources and the Faculty of Chemical and Food Engineering at Bahir Dar University, Bahir Dar, Ethiopia, for facilitating laboratory testing. Additionally, heartfelt gratitude is extended to Adama Science and Technology University, Adama, Ethiopia, and the Ethiopian Geological Survey Institute, Addis Ababa, Ethiopia, for their invaluable assistance in conducting laboratory experiments.

Conflicts of Interest: The authors declare no conflicts of interest.

References

1. Krishna, N.K.; Sandeep, S.; Mini, K.M. Study on concrete with partial replacement of cement by rice husk ash. In *IOP Conference Series: Materials Science and Engineering*; IOP Publishing: Bristol, UK, 2016.
2. Bouchima, L.; Rouis, M.J.; Choura, M. Correlation of Ultrasound Pulse Velocity with Mechanical Properties and Water Absorption in Phosphogypsum-wade Sand-Lime-Cement Building Bricks produced under a static compaction of 20 MPa. *Int. J. Latest Technol. Eng. Manag. Appl. Sci. IJLTEMAS* **2015**, *4*, 1–5.
3. Cosentino, I.; Liendo, F.; Arduino, M.; Restuccia, L.; Bensaid, S.; Deorsola, F.; Ferro, G.A. Nano CaCO₃ particles in cement mortars towards developing a circular economy in the cement industry. *Procedia Struct. Integr.* **2020**, *26*, 155–165.
4. Thwe, E.; Khatiwada, D.; Gasparatos, A. Life cycle assessment of a cement plant in Naypyitaw, Myanmar. *Clean. Environ. Syst.* **2021**, *2*, 100007.
5. Worku, M.A.; Taffese, W.Z.; Hailemariam, B.Z.; Yehualaw, M.D. Cow dung ash in mortar: An experimental study. *Appl. Sci.* **2023**, *13*, 6218. [[CrossRef](#)]
6. Getachew, E.M.; Yifru, B.W.; Taffese, W.Z.; Yehualaw, M.D. Enhancing mortar properties through thermoactivated recycled concrete cement. *Buildings* **2023**, *13*, 2209. [[CrossRef](#)]
7. Yehualaw, M.D.; Alemu, M.; Hailemariam, B.Z.; Vo, D.H.; Taffese, W.Z. Aquatic weed for concrete sustainability. *Sustainability* **2022**, *14*, 15501. [[CrossRef](#)]
8. Nebiyu, W.M.; Nuramo, D.A.; Ketema, A.F. Experimental Study of Recycled Aggregate Concrete Produced from Recycled Fine Aggregate. In Proceedings of the Advances of Science and Technology: 9th EAI International Conference, ICAST 2021, Hybrid Event, Bahir Dar, Ethiopia, 27–29 August 2021; Proceedings, Part II. Springer: Cham, Switzerland, 2022.
9. Rajput, J.; Yadav, R.; Chandak, R. The effect of rice husk ash used as supplementary cementing material on strength of mortar. *Int. J. Eng. Res. Appl.* **2013**, *3*, 133–136.
10. Hailemariam, B.Z.; Yehualaw, M.D.; Taffese, W.Z.; Vo, D.H. Optimizing Alkali-Activated Mortars with Steel Slag and Eggshell Powder. *Buildings* **2024**, *14*, 2336. [[CrossRef](#)]
11. Nega, D.M.; Yifru, B.W.; Taffese, W.Z.; Ayele, Y.K.; Yehualaw, M.D. Impact of partial replacement of cement with a blend of marble and granite waste powder on mortar. *Appl. Sci.* **2023**, *13*, 8998. [[CrossRef](#)]
12. Endale, S.; Taffese, W.Z.; Vo, D.H.; Yehualaw, M.D. Rice husk ash in concrete. *Sustainability* **2023**, *15*, 137.
13. Ephraim, M.E.; Akeke, G.A.; Ukpata, J.O. Compressive strength of concrete with rice husk ash as partial replacement of ordinary Portland cement. *Sch. J. Eng. Res.* **2012**, *1*, 32–36.
14. Ali, T.; Saand, A.; Bangwar, D.K.; Buller, A.S.; Ahmed, Z. Mechanical and durability properties of aerated concrete incorporating rice husk ash (RHA) as partial replacement of cement. *Crystals* **2021**, *11*, 604. [[CrossRef](#)]
15. Zareei, S.A.; Ameri, F.; Dorostkar, F.; Ahmadi, M. Rice husk ash as a partial replacement of cement in high strength concrete containing micro silica: Evaluating durability and mechanical properties. *Case Stud. Constr. Mater.* **2017**, *7*, 73–81.
16. Lezzerini, M.; Luti, L.; Aquino, A.; Gallelo, G.; Pagnotta, S. Effect of marble waste powder as a binder replacement on the mechanical resistance of cement mortars. *Appl. Sci.* **2022**, *12*, 4481. [[CrossRef](#)]
17. Chandrakar, R.; Singh, A. Cement replacement in concrete with marble dust powder. *Int. Res. J. Eng. Technol.* **2017**, *4*, 1409–1411.

18. Bakar, R.A.; Yahya, R.; Gan, S.N. Production of high purity amorphous silica from rice husk. *Procedia Chem.* **2016**, *19*, 189–195.
19. Ramezani-pour, A.; Pourbeik, P.; Mahdikhani, M.; Moodi, F. Mechanical properties and durability of concretes containing rice husk ash as supplementary cementing material. In Proceedings of the 2nd International Conference on Sustainable Construction Materials and Technologies, Ancona, Italy, 28–30 June 2010.
20. Alex, J.; Dhanalakshmi, J.; Ambedkar, B. Experimental investigation on rice husk ash as cement replacement on concrete production. *Constr. Build. Mater.* **2016**, *127*, 353–362.
21. Neville, A.M.; Brooks, J.J. *Concrete Technology*; Longman Scientific & Technical England: London, UK, 1987; Volume 438.
22. *ASTM C618-22*; Standard Specification for Coal Fly Ash and Raw or Calcined Natural Pozzolan for Use in Concrete. ASTM International: West Conshohocken, PA, USA, 2022.
23. Snellings, R.; Mertens, G.; Elsen, J. Supplementary cementitious materials. *Rev. Mineral. Geochem.* **2012**, *74*, 211–278.
24. Zain, M.F.M.; Islam, M.N.; Mahmud, F.; Jamil, M. Production of rice husk ash for use in concrete as a supplementary cementitious material. *Constr. Build. Mater.* **2011**, *25*, 798–805.
25. *ASTM C33-07*; Standard Specification for Concrete Aggregates. ASTM International: West Conshohocken, PA, USA, 2008.
26. *ASTM C29*; Standard Test Method for Bulk Density (Unit Weight) and Voids in Aggregate. ASTM International: West Conshohocken, PA, USA, 2008.
27. *ASTM C128-07*; Standard Test Method for Density, Relative Density (Specific Gravity), and Absorption of Fine Aggregate. ASTM International: West Conshohocken, PA, USA, 2007.
28. *ASTM C566-97*; Standard Test Method for Total Evaporable Moisture Content of Aggregate by Drying. ASTM International: West Conshohocken, PA, USA, 2013.
29. *ASTM C117-04*; Standard Test Method for Materials Finer than 75- μm (No. 200) Sieve in Mineral Aggregates by Washing. ASTM International: West Conshohocken, PA, USA, 2003.
30. *ASTM C109/C109M-02*; Standard Test Method for Compressive Strength of Hydraulic Cement Mortars. ASTM International: West Conshohocken, PA, USA, 2002.
31. *ASTM C187*; Standard Test Method for Amount of Water Required for Normal Consistency of Hydraulic Cement Paste. ASTM International: West Conshohocken, PA, USA, 2011.
32. *ASTM C191-08*; Standard Test Methods for Time of Setting of Hydraulic Cement by Vicat Needle. ASTM International: West Conshohocken, PA, USA, 2008.
33. *ASTM C1437*; Standard Test Method for Flow of Hydraulic Cement Mortar. ASTM International: West Conshohocken, PA, USA, 2001.
34. *ASTM C642*; Standard Test Method for Density, Absorption, and Voids in Hardened Concrete. ASTM International: West Conshohocken, PA, USA, 2013.
35. *ASTM C1012/C1012M*; Standard Test Method for Length Change of Hydraulic Cement Mortars Exposed to a Sulfate Solution. ASTM International: West Conshohocken, PA, USA, 2018.
36. *ASTM C597-16*; Standard Test Method for Pulse Velocity through Concrete. ASTM International: West Conshohocken, PA, USA, 2018.
37. Mohseni, E.; Yazdi, M.A.; Miyandehi, B.M.; Zadshir, M.; Ranjbar, M.M. Combined effects of metakaolin, rice husk ash, and polypropylene fiber on the engineering properties and microstructure of mortar. *J. Mater. Civ. Eng.* **2017**, *29*, 04017025.
38. Thiedeitz, M.; Ostermaier, B.; Kränkel, T. Rice husk ash as an additive in mortar—Contribution to microstructural, strength and durability performance. *Resour. Conserv. Recycl.* **2022**, *184*, 106389. [[CrossRef](#)]
39. Givi, A.N.; Rashid, S.A.; Aziz, F.N.A.; Salleh, M.A.M. Contribution of rice husk ash to the properties of mortar and concrete: A review. *J. Am. Sci.* **2010**, *6*, 157–165.
40. Madhava Krishna Reddy, G.; Sreenivasulu Gopu, M.G.K.; Sashidhar, C. Experimental Studies on Blended Concrete with Chemically Cured Coarse Aggregate. *Int. J. Eng. Technol. Sci. Res.* **2017**, *4*, 202–203.
41. Mounika, G.; Baskar, R.; Sri Kalyana Rama, J. Rice husk ash as a potential supplementary cementitious material in concrete solution towards sustainable construction. *Innov. Infrastruct. Solut.* **2022**, *7*, 51.
42. Srinivasreddy, A.B.; McCarthy, T.; Lume, E. Effect of rice husk ash on workability and strength of concrete. In Proceedings of the 26th Biennial Concrete Institute of Australia’s National Conference, Gold Coast, Australia, 16–18 October 2013.
43. Pathan, V.G.; Pathan, M.G. Feasibility and need of use of waste marble powder in concrete production. *IOSR J. Mech. Civ. Eng.* **2014**, *6*, 23–26.
44. Rao, B.K. Study on marble powder as partial replacement of cement in normal compacting concrete. *IOSR J. Mech. Civ. Eng. (IOSR-JMCE)* **2016**, *13*, 1–5.
45. De Sensale, G.R. Effect of rice-husk ash on durability of cementitious materials. *Cem. Concr. Compos.* **2010**, *32*, 718–725. [[CrossRef](#)]
46. Ulubeyli, G.C.; Artir, R. Properties of hardened concrete produced by waste marble powder. *Procedia Soc. Behav. Sci.* **2015**, *195*, 2181–2190.

47. Meziani, M.; Chelouah, N.; Amiri, O.; Leklou, N. Blended cement hydration assessment by thermogravimetric analysis and isothermal calorimetry. In Proceedings of the MATEC Web of Conferences, Reykjavik, Iceland, 12 August 2018; EDP Sciences: Les Ulis, France, 2018.
48. Zhou, Z.; Sofi, M.; Lumantarna, E.; San Nicolas, R.; Hadi Kusuma, G.; Mendis, P. Strength development and thermogravimetric investigation of high-volume fly ash binders. *Materials* **2019**, *12*, 3344. [[CrossRef](#)]
49. Wang, W.; Meng, Y.; Wang, D. Effect of rice husk ash on high-temperature mechanical properties and microstructure of concrete. *Kem. U Ind. Časopis Kemičara I Kem. Inženjera Hrvat.* **2017**, *66*, 157–164.
50. Alarcon-Ruiz, L.; Platret, G.; Massieu, E.; Ehlacher, A. The use of thermal analysis in assessing the effect of temperature on a cement paste. *Cem. Concr. Res.* **2005**, *35*, 609–613. [[CrossRef](#)]
51. Ahmed, A.; Ameer, S.; Abbas, S.; Abbass, W.; Razzaq, A.; Mohamed, A.M.; Mohamed, A. Effectiveness of ternary blend incorporating rice husk ash, silica fume, and cement in preparing ASR resilient concrete. *Materials* **2022**, *15*, 2125. [[CrossRef](#)] [[PubMed](#)]
52. Amaran, R.; Ravi, R. Effect of cactus on the rheological properties of cement. *Int. J. Chem. Sci.* **2016**, *14*, 203–210.
53. Horgnies, M.; Chen, J.; Bouillon, C. Overview about the use of Fourier transform infrared spectroscopy to study cementitious materials. *WIT Trans. Eng. Sci.* **2013**, *77*, 251–262.
54. Malathy, R.; Shanmugam, R.; Chung, I.M.; Kim, S.H.; Prabakaran, M. Mechanical and microstructural properties of composite mortars with lime, silica fume and rice husk ash. *Processes* **2022**, *10*, 1424. [[CrossRef](#)]
55. Luo, Y.-B.; Zhang, Y.-J. Investigation of sticky-rice lime mortar of the Horse Stopped Wall in Jiange. *Herit. Sci.* **2013**, *1*, 26. [[CrossRef](#)]
56. Ylmen, R.; Jäglid, U. Carbonation of Portland cement studied by diffuse reflection Fourier transform infrared spectroscopy. *Int. J. Concr. Struct. Mater.* **2013**, *7*, 119–125. [[CrossRef](#)]
57. Thomas, B.S. Green concrete partially comprised of rice husk ash as a supplementary cementitious material—A comprehensive review. *Renew. Sustain. Energy Rev.* **2018**, *82*, 3913–3923. [[CrossRef](#)]
58. Varadharajan, S.; Jaiswal, A.; Verma, S. Assessment of mechanical properties and environmental benefits of using rice husk ash and marble dust in concrete. In *Structures*; Elsevier: Amsterdam, The Netherlands, 2020.
59. Chanu, N.M.; Devi, T.K. Contribution of rice husk ash to the properties of cement mortar and concrete. *Int. J. Eng. Res. Technol.* **2013**, *2*, 1–7.
60. Ibrahim, I.A.; Ahmad, E.; Dulawat, S.; Garko, M.N.; Ibrahim, U.S.; Ubayi, S.S.; Ibrahim, M.A. A review on the impact of rice husk ash and marble waste powder on concrete properties. *Int. J. Mech. Civ. Eng.* **2024**, *7*, 145–159. [[CrossRef](#)]
61. Shaladi, R.J.; Johari, M.A.M.; Ahmad, Z.A.; Mijarsh, M.J. The influence of palm oil fuel ash heat treatment on the strength activity, porosity, and water absorption of cement mortar. *Environ. Sci. Pollut. Res.* **2022**, *29*, 72493–72514.
62. Nugroho, M.S.; Ma'arif, F.; Widodo, S.; Rachmi, D.; Fajriani, Q.; Suryadwanti, N.; Setiawan, W. The effect of mortar mixture variations on the compressive strength and ultrasonic pulse velocity. *INERSIA Informati Dan Ekspose Has. Ris. Tek. Sipil Dan Arsit.* **2022**, *18*, 225–234. [[CrossRef](#)]

Disclaimer/Publisher's Note: The statements, opinions and data contained in all publications are solely those of the individual author(s) and contributor(s) and not of MDPI and/or the editor(s). MDPI and/or the editor(s) disclaim responsibility for any injury to people or property resulting from any ideas, methods, instructions or products referred to in the content.